



VICTORIA UNIVERSITY
MELBOURNE AUSTRALIA

Analysis of heat and mass transfer by CFD for performance enhancement in direct contact membrane distillation

This is the Accepted version of the following publication

Yu, Hui, Yang, Xing, Wang, Rong and Fane, Anthony G (2012) Analysis of heat and mass transfer by CFD for performance enhancement in direct contact membrane distillation. *Journal of Membrane Science*, 405-406. pp. 38-47. ISSN 0376-7388

The publisher's official version can be found at
<http://www.sciencedirect.com/science/article/pii/S037673881200141X>
Note that access to this version may require subscription.

Downloaded from VU Research Repository <https://vuir.vu.edu.au/25292/>

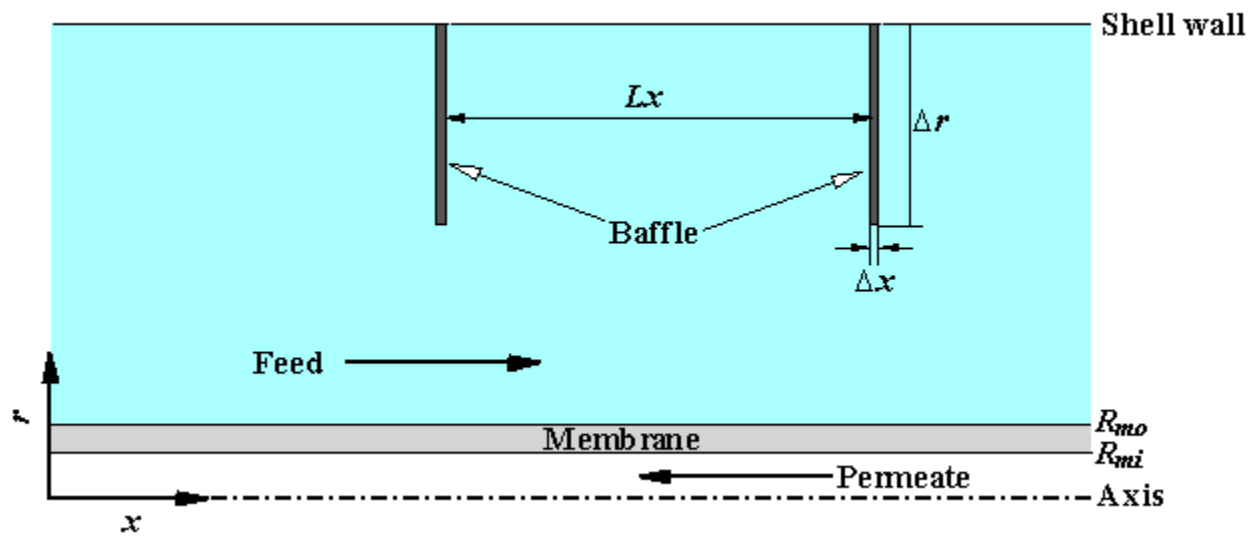


Fig. 1. Schematic of axially-symmetry single fiber module in CFD simulating domain

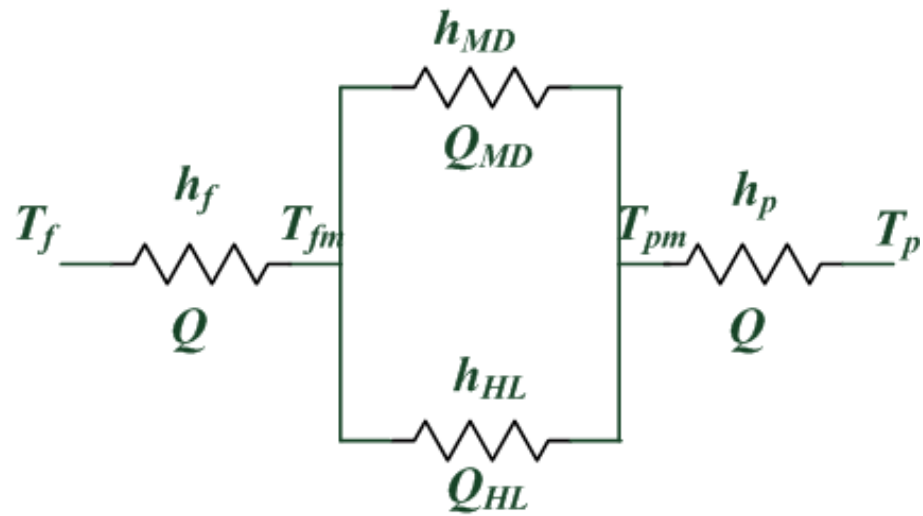


Fig. 2. Schematic of heat transfer process in MD

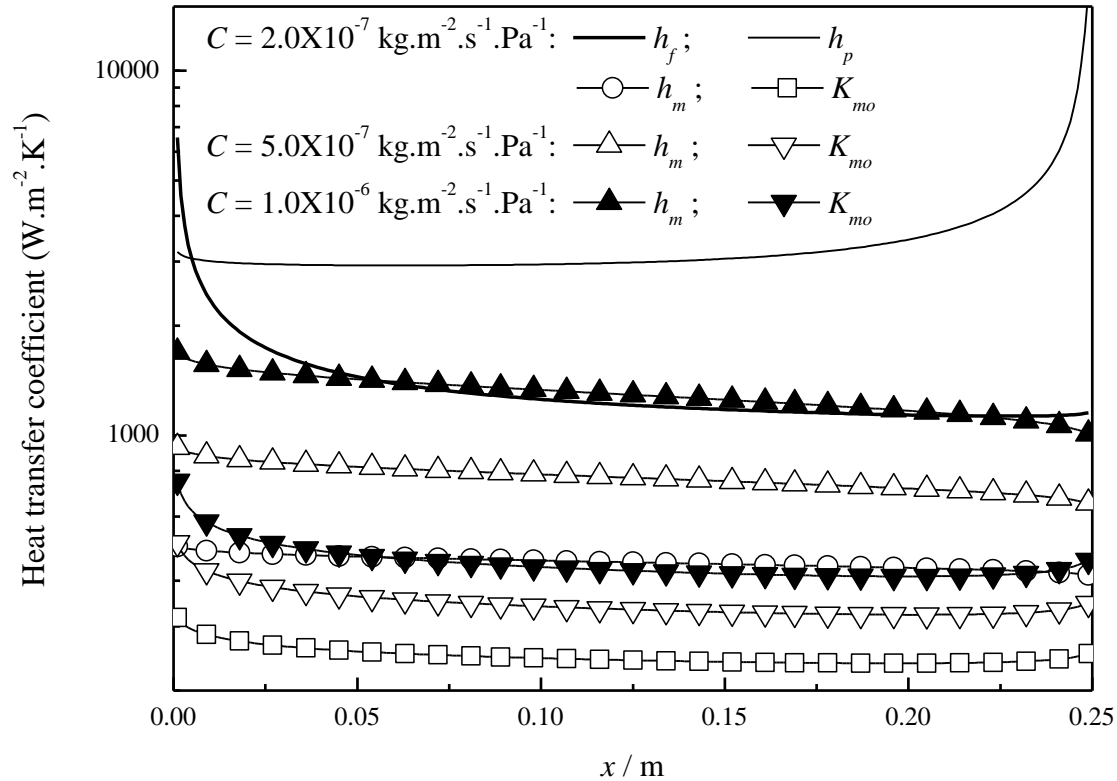


Fig. 3. Heat-transfer coefficient distributions along the module length for membranes with different C values ($T_{fi} = 327.2$ K, $T_{pi} = 294.0$ K, $u_{fi} = 0.06$ m·s⁻¹, $u_{pi} = 0.417$ m·s⁻¹, $C = 2.0 \times 10^{-7}$ to 1.0×10^{-6} kg·m⁻²·s⁻¹·Pa⁻¹)

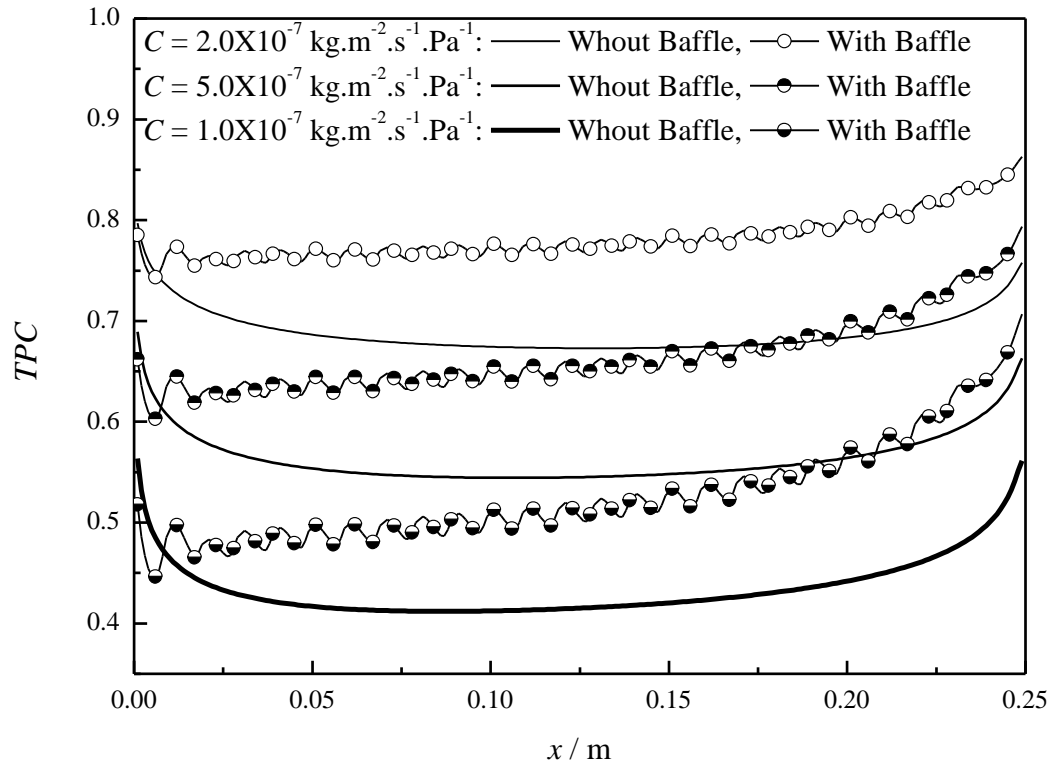


Fig. 4. *TPC* distributions along the module length for non-baffled and baffled modules with membranes of different *C* values
 ($T_{fi} = 327.2 \text{ K}$, $T_{pi} = 294.0 \text{ K}$, $u_{fi} = 0.06 \text{ m} \cdot \text{s}^{-1}$, $u_{pi} = 0.417 \text{ m} \cdot \text{s}^{-1}$, $C = 2.0 \times 10^{-7}$ to $1.0 \times 10^{-6} \text{ kg} \cdot \text{m}^{-2} \cdot \text{s}^{-1} \cdot \text{Pa}^{-1}$)

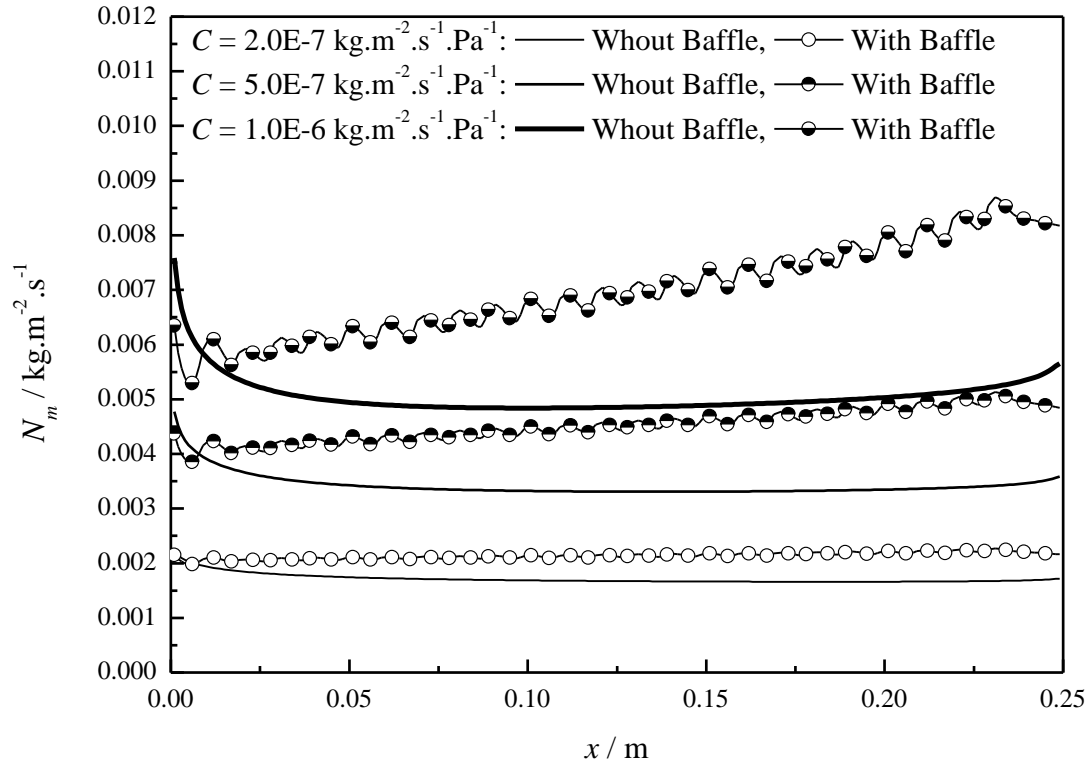


Fig. 5. N_m distributions along the module length for non-baffled and baffled modules with membranes of different C values

($T_{fi} = 327.2 \text{ K}$, $T_{pi} = 294.0 \text{ K}$, $u_{fi} = 0.06 \text{ m}\cdot\text{s}^{-1}$, $u_{pi} = 0.417 \text{ m}\cdot\text{s}^{-1}$, $C = 2.0 \times 10^{-7}$ to $1.0 \times 10^{-6} \text{ kg}\cdot\text{m}^{-2}\cdot\text{s}^{-1}\cdot\text{Pa}^{-1}$)

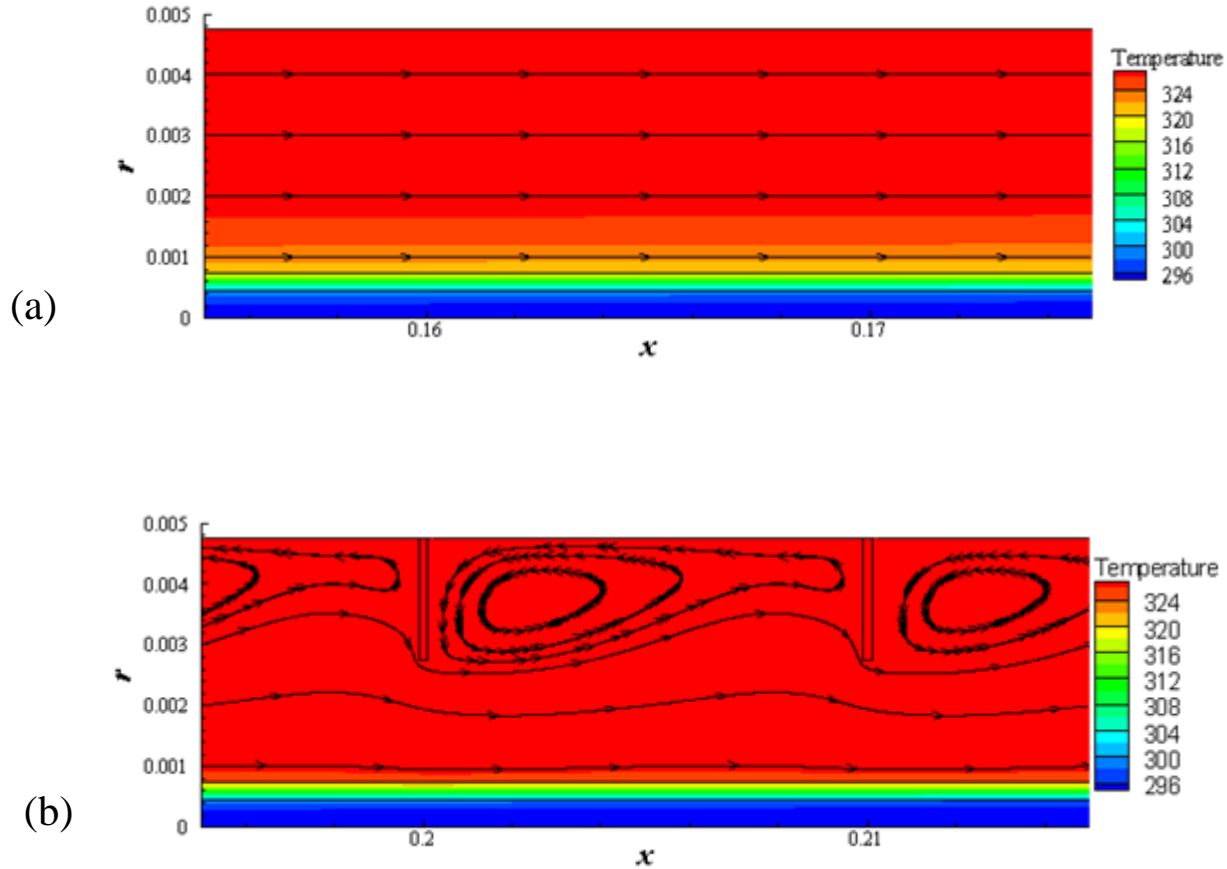


Fig. 6. Temperature distributions and flow fields at the shell side of 0.25m modules (local snapshots)

(a) without baffles; (b) with baffles

$$(T_{fi} = 327.2 \text{ K}, T_{pi} = 294.0 \text{ K}, u_{fi} = 0.06 \text{ m}\cdot\text{s}^{-1}, u_{pi} = 0.417 \text{ m}\cdot\text{s}^{-1}, C = 2.0 \times 10^{-7} \text{ kg}\cdot\text{m}^{-2}\cdot\text{s}^{-1}\cdot\text{Pa}^{-1})$$

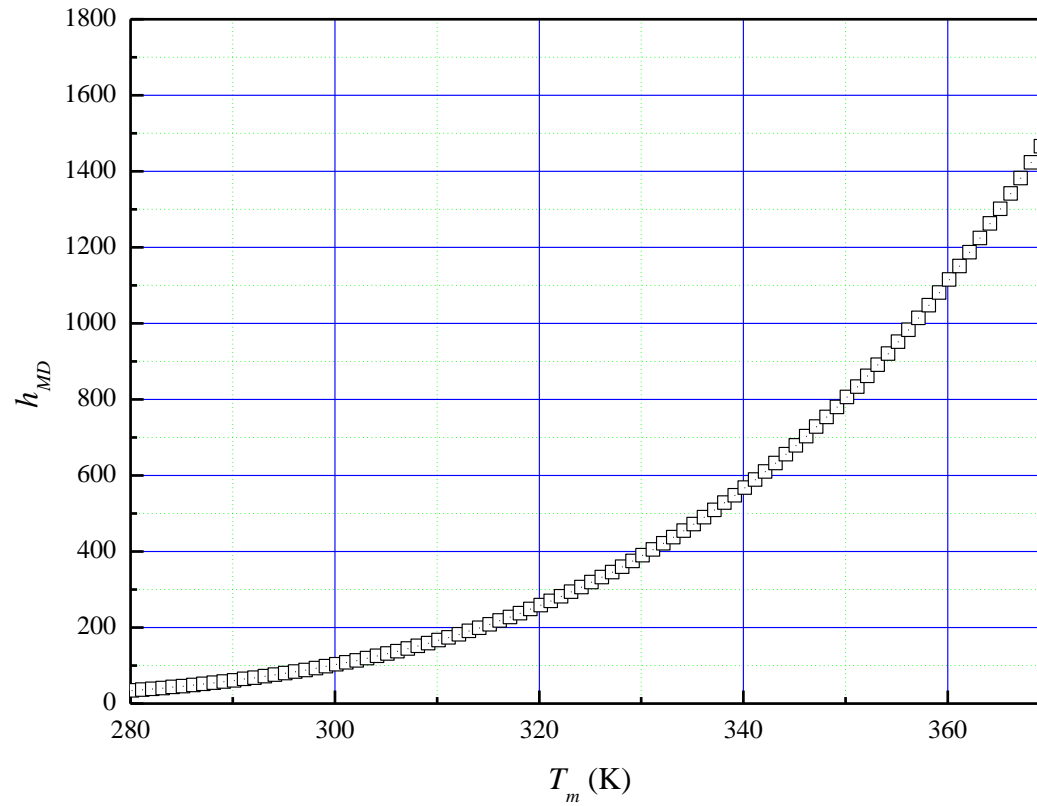


Fig. 7. h_{MD} vs. membrane temperature T_m with $C = 2.0 \times 10^{-7} \text{ kg} \cdot \text{m}^{-2} \cdot \text{s}^{-1} \cdot \text{Pa}^{-1}$

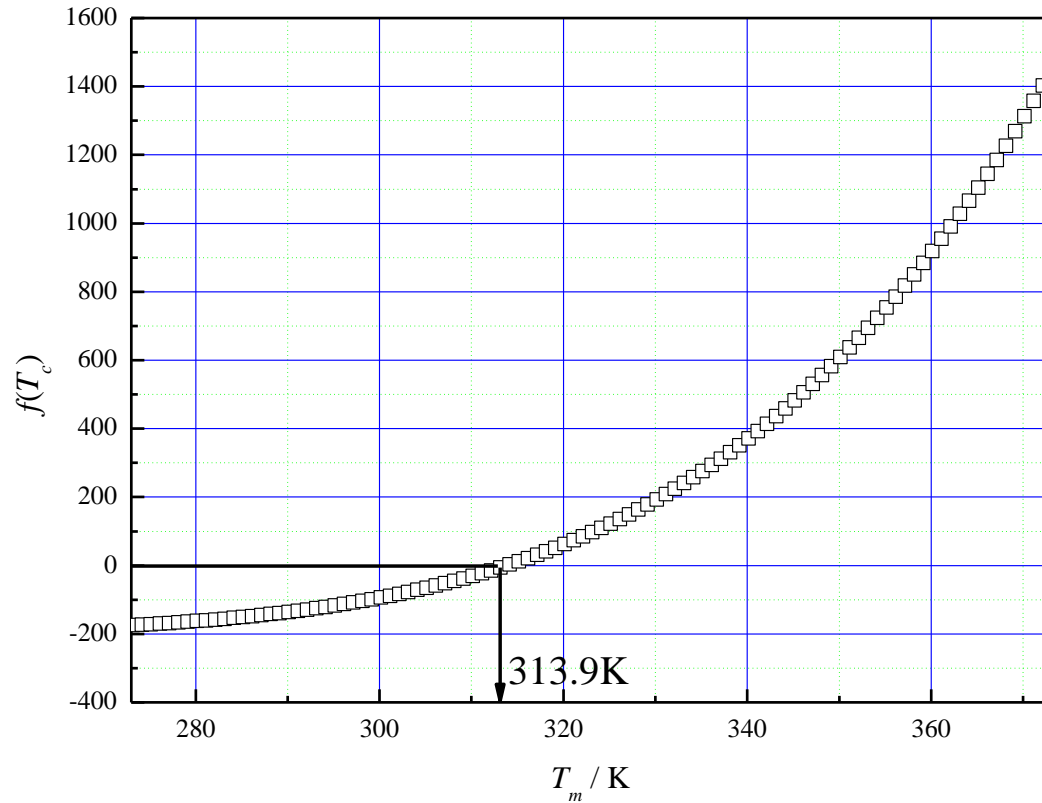


Fig. 8. Function $f(T_c)$ at varied membrane temperatures T_m with $C = 2.0 \times 10^{-7} \text{ kg} \cdot \text{m}^{-2} \cdot \text{s}^{-1} \cdot \text{Pa}^{-1}$

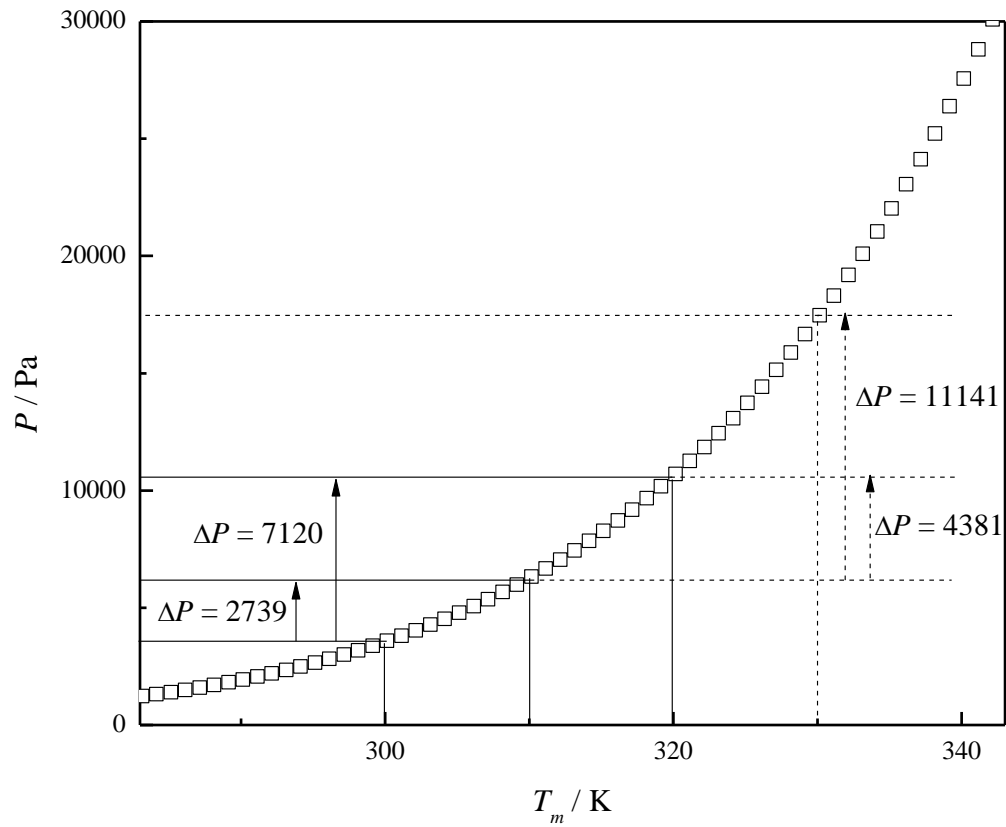


Fig. 9. The distribution of saturated vapor pressure difference ΔP at various membrane temperatures T_m

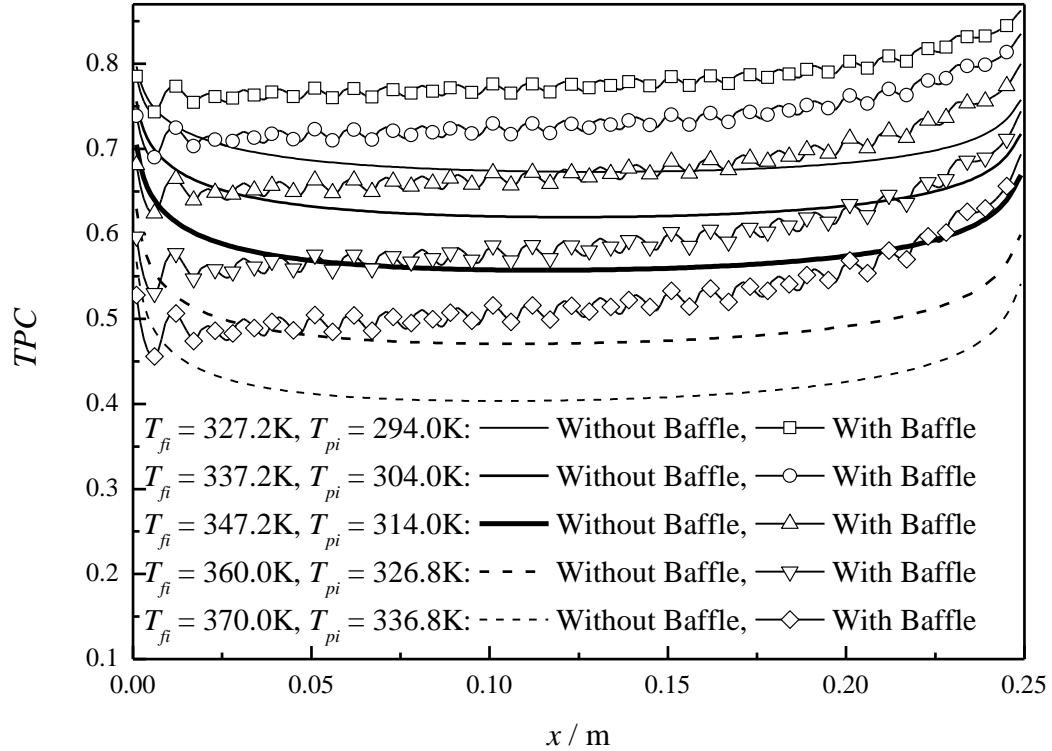
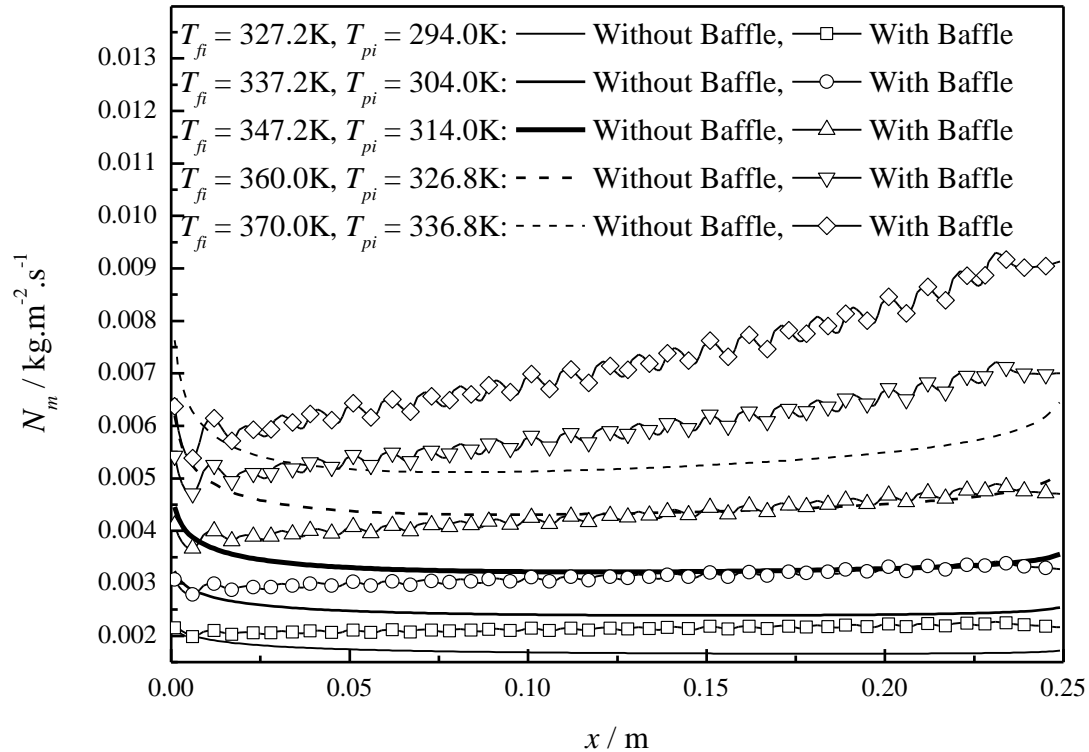


Fig. 10. TPC distribution along the module length for non-baffled and baffled modules at varied feed/permeate inlet temperatures with a constant temperature difference ($\Delta T_{in}=33.2\text{ K}$, $u_{fi}=0.06\text{ m}\cdot\text{s}^{-1}$, $u_{pi}=0.417\text{ m}\cdot\text{s}^{-1}$, $C=2.0\times 10^{-7}\text{ kg}\cdot\text{m}^{-2}\cdot\text{s}^{-1}\cdot\text{Pa}^{-1}$)

(a) N_m distribution along the module length



(b) Local mass fluxes N_m comparison ($x=0.125m$)

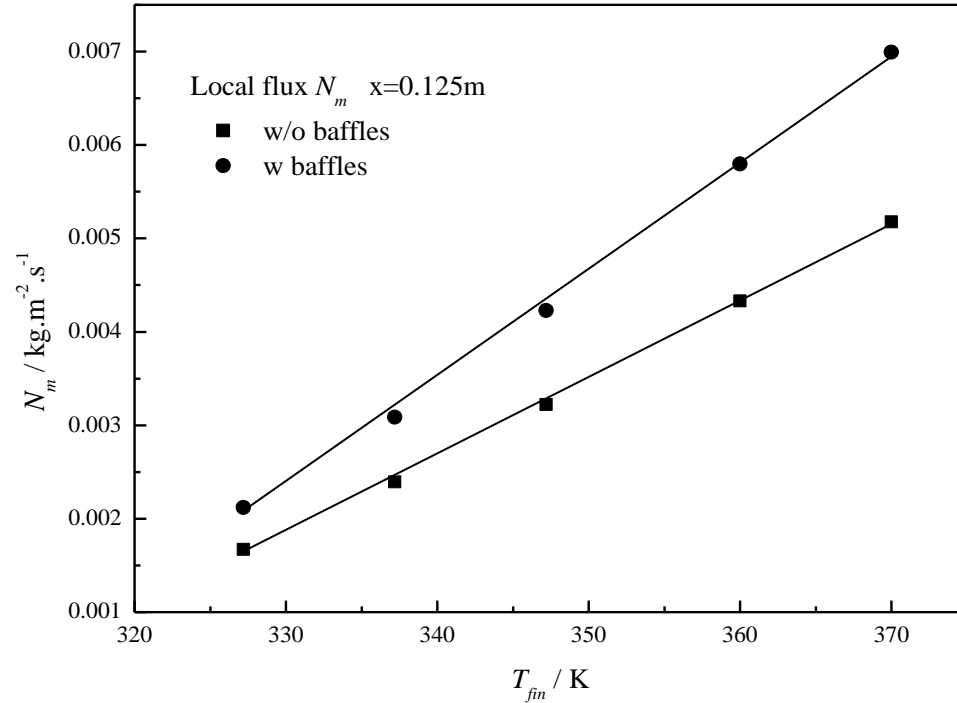


Fig. 11. N_m results for non-baffled and baffled modules at varied feed/permeate inlet temperatures with a constant temperature difference ΔT_{in}
 (a) N_m distribution along the module length; (b) Local mass fluxes N_m comparison $x=0.125m$
 ($\Delta T_{in}=33.2$ K, $u_{fi}=0.0602$ m \cdot s $^{-1}$, $u_{pi}=0.417$ m \cdot s $^{-1}$, $C=2.0\times 10^{-7}$ kg \cdot m $^{-2}\cdot$ s $^{-1}\cdot$ Pa $^{-1}$)

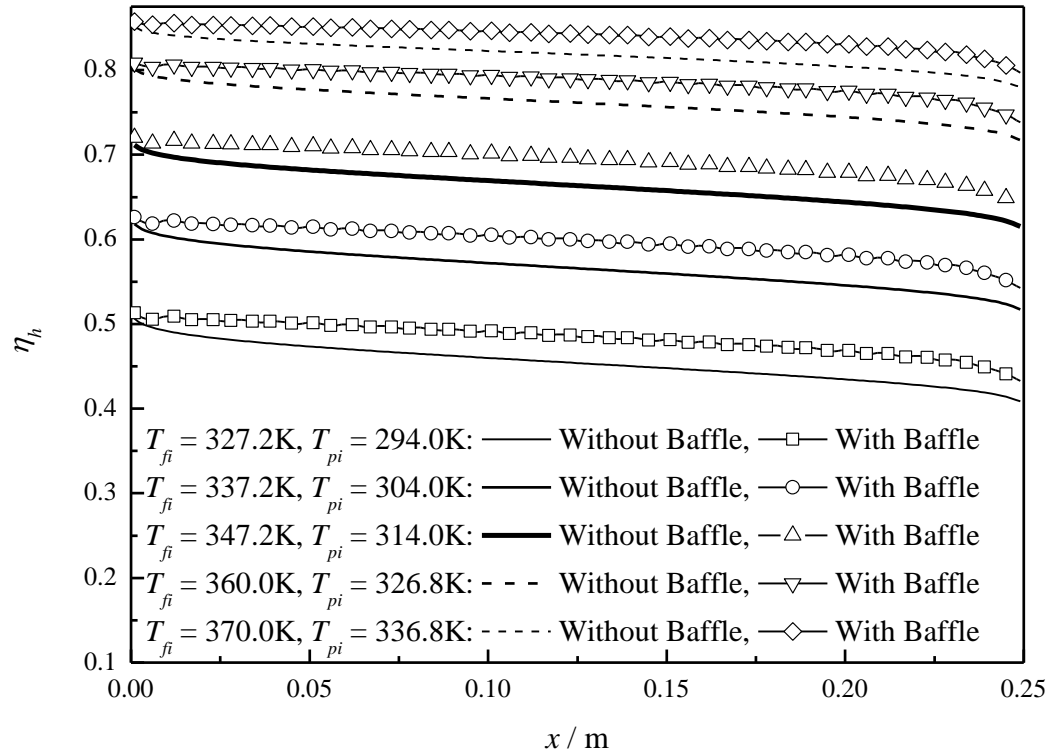


Fig. 12. η_h distribution along the module length for non-baffled and baffled modules at varied feed/permeate inlet temperatures with a constant temperature difference ($\Delta T_{in}=33.2\text{ K}$, $u_{fi}=0.06\text{ m}\cdot\text{s}^{-1}$, $u_{pi}=0.417\text{ m}\cdot\text{s}^{-1}$, $C=2.0\times 10^{-7}\text{ kg}\cdot\text{m}^{-2}\cdot\text{s}^{-1}\cdot\text{Pa}^{-1}$)

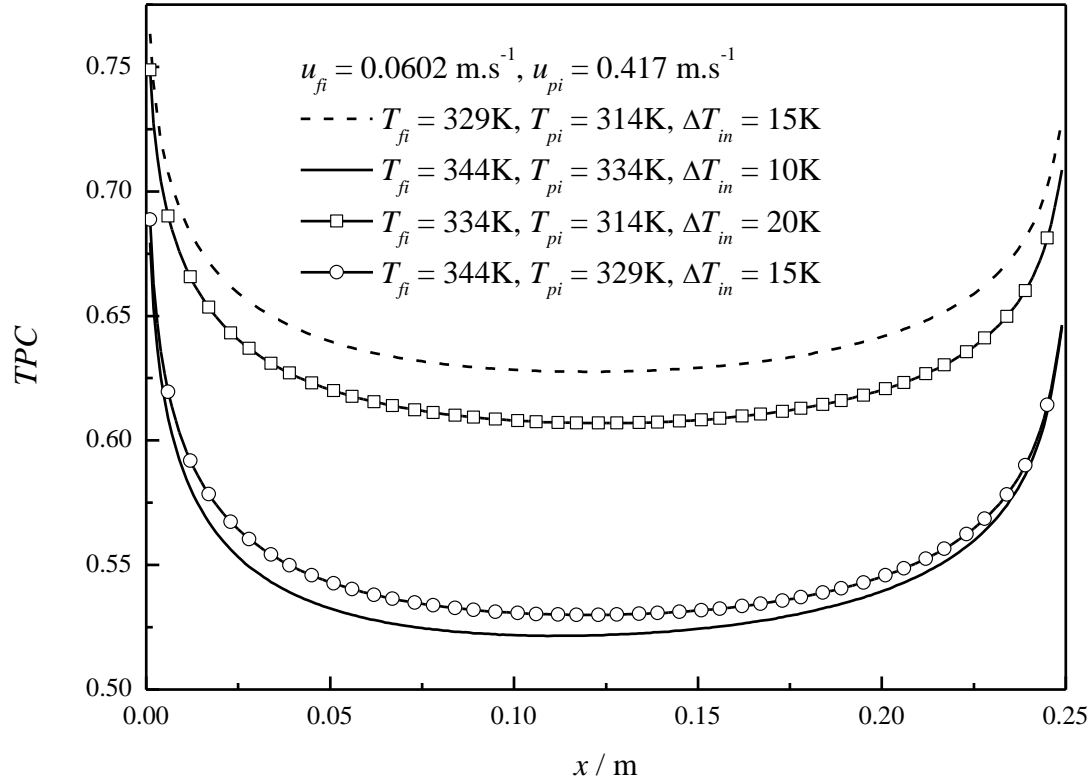


Fig. 13. *TPC* distributions along the module length at varied feed/permeate inlet temperatures T_{fi}/T_{pi} and temperature differences ΔT_{in} ($u_{fi}=0.06 \text{ m}\cdot\text{s}^{-1}, u_{pi}= 0.417 \text{ m}\cdot\text{s}^{-1}, C = 2.0 \times 10^{-7} \text{ kg}\cdot\text{m}^{-2}\cdot\text{s}^{-1}\cdot\text{Pa}^{-1}$)

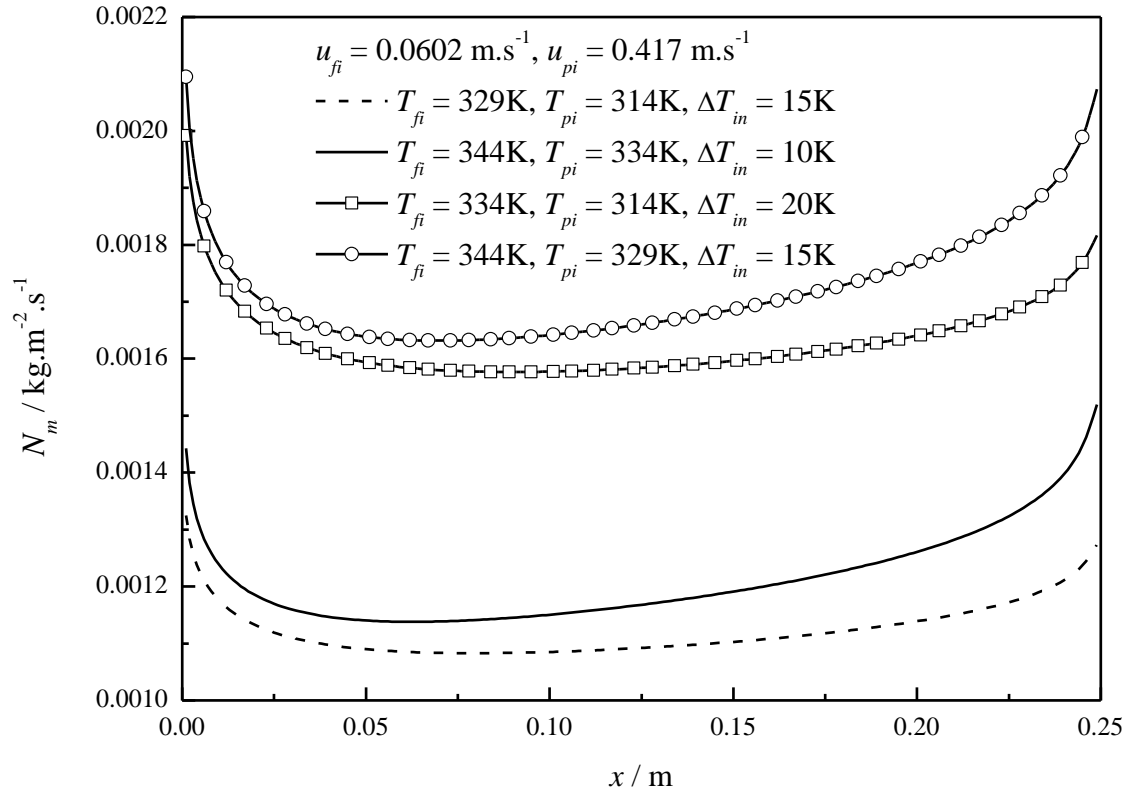


Fig. 14. N_m distributions along the module length at varied feed/permeate inlet temperatures T_{fi}/T_{pi} and temperature differences ΔT_{in} ($u_{fi}=0.06 \text{ m}\cdot\text{s}^{-1}$, $u_{pi}=0.417 \text{ m}\cdot\text{s}^{-1}$, $C = 2.0 \times 10^{-7} \text{ kg}\cdot\text{m}^{-2}\cdot\text{s}^{-1}\cdot\text{Pa}^{-1}$)

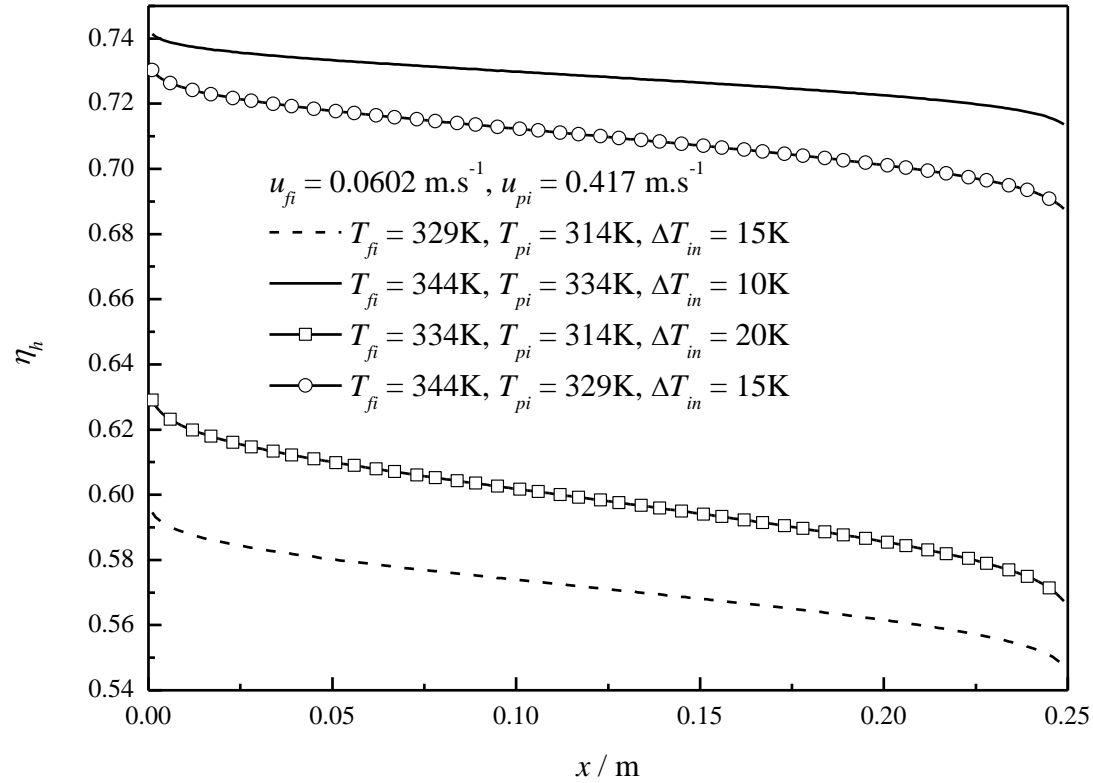


Fig. 15. η_h distributions along the module length at varied feed/permeate inlet temperatures T_{fi}/T_{pi} and temperature differences ΔT_{in}
 ($u_{fi}=0.06 \text{ m}\cdot\text{s}^{-1}$, $u_{pi}= 0.417 \text{ m}\cdot\text{s}^{-1}$, $C = 2.0 \times 10^{-7} \text{ kg}\cdot\text{m}^{-2}\cdot\text{s}^{-1}\cdot\text{Pa}^{-1}$)

Table. 1. The temperature comparison of experimental data and simulation results
 ($u_{fi}=0.06 \text{ m}\cdot\text{s}^{-1}$, $u_{pi}=0.417 \text{ m}\cdot\text{s}^{-1}$, $C=2.0\times 10^{-7} \text{ kg}\cdot\text{m}^{-2}\cdot\text{s}^{-1}\cdot\text{Pa}^{-1}$)

L (m)		T_{fi} (K)	T_{fo} (K)	Error (%)	T_{pi} (K)	T_{po} (K)	Error (%)
0.25	Exp.	327.2	325.7	-	294.0	301.4	-
	Sim.	-	325.9	0.0614			
0.25	Exp.	333.9	331.6	-	294.4	302.8	-
	Sim.	-	332.5	-0.271			
0.25	Exp.	334.8	333.8	-	312.8	317.7	-
	Sim.	-	333.6	-0.0599			
0.25	Exp.	337.6	334.8	-	294.3	304.1	-
	Sim.	-	336.2	0.418			
0.25	Exp.	337.6	336.4	-	304.0	311.1	-
	Sim.	-	336.3	-0.0297			